Principal Diffusion Direction in Peritumoral Fiber Tracts

Color Map Patterns and Directional Statistics

AARON S. FIELD,[a,b] YU-CHIEN WU,[c] AND ANDREW L. ALEXANDER[c,d]

Departments of [a]Radiology, [b]Biomedical Engineering, [c]Medical Physics, and [d]Psychiatry, University of Wisconsin–Madison, Madison, Wisconsin, USA

ABSTRACT: The ability of diffusion tensor imaging (DTI) to probe the ultrastructural properties of biological tissues presents new possibilities for DTI-based tissue characterization, with the potential for greater pathologic specificity than conventional imaging methods. This is urgently needed in the diagnosis and treatment of cerebral neoplasms, where clinical decisions depend on the ability to discriminate tumor-involved from uninvolved tissue, a major shortcoming of conventional imaging. Several investigators have attempted to make this determination on the basis of the apparent diffusion coefficient (ADC) or the fractional anisotropy (FA), with mixed results. The directionally encoded color map, with hues reflecting tensor orientation and intensity weighted by FA, provides an aesthetic and informative summary of DTI features throughout the brain in an easily interpreted format. The use of these maps is becoming increasingly common in both basic and clinical research, as well as in purely clinical settings. These examples serve to demonstrate our approach to the quantitation of regional diffusion tensor distributions using directional statistical methods.

KEYWORDS: diffusion tensor imaging (DTI); apparent diffusion coefficient (ADC); fractional anisotropy (FA); color map; direction; edema; glioma

INTRODUCTION

The ability of diffusion tensor imaging (DTI) to probe the ultrastructural properties of biological tissues presents new possibilities for DTI-based tissue characterization, with the potential for greater pathologic specificity than conventional imaging methods. This is urgently needed in the diagnosis and treatment of cerebral neoplasms, where clinical decisions depend on the ability to discriminate tumor-involved from uninvolved tissue, a major shortcoming of conventional imaging. For example, it is frequently impossible to determine whether T2 prolongation in the white matter (WM) surrounding a glioma represents tumor infiltration or bland (tumor-free) edema. Several investigators have attempted to make this determination on the basis of the

Address for correspondence: Aaron S. Field, M.D., Ph.D., Assistant Professor, Department of Radiology, University of Wisconsin, 600 Highland Avenue, CSC E3/311, Madison, WI 53792. Voice: 608-263-7952; fax: 608-265-4152.
as.field@hosp.wisc.edu

Ann. N.Y. Acad. Sci. 1064: 193–201 (2005).
doi: 10.1196/annals.1340.037

apparent diffusion coefficient (ADC)[1–12] and/or the fractional anisotropy (FA),[5,9–11] with mixed results. The most recent studies employing the most sophisticated DTI methodology have revealed a tendency for tumor infiltration to cause greater FA reductions than edema.[5,10,11] However, these differences have been small and they may prove less significant to decision-making in individual patients than to statistical comparisons of sizable groups. We have observed substantial overlap of FA distributions between infiltrating gliomas and bland edema.[13]

The ADC and FA constitute just a fraction of the information available from the diffusion tensor. The examination of individual eigenvalues, as well as measures of

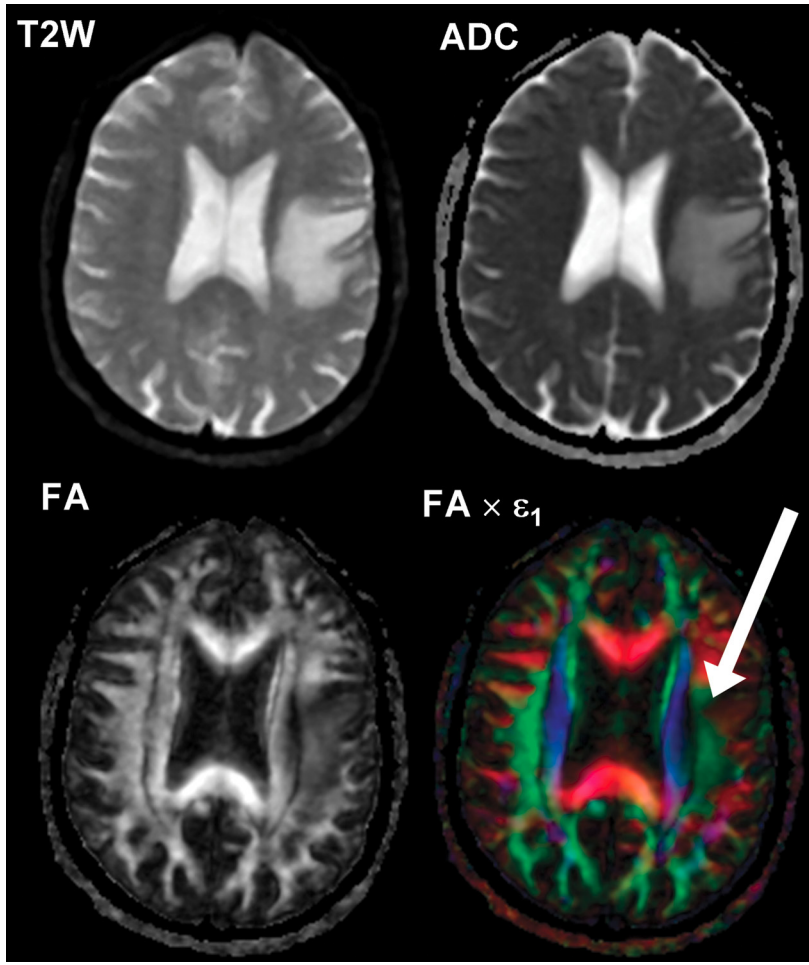

FIGURE 1. T2-weighted (T2W), ADC, FA, and FA-weighted, directionally encoded DTI color maps ($FA \times \varepsilon_1$) in a patient with a region of bland (tumor-free) vasogenic edema involving the left corona radiata and superior longitudinal fasciculus.[16] This region shows reduced FA, but normal color hues (*arrow*).

tensor shape and orientation, opens many new possibilities for tissue characterization. For example, the major eigenvalue of the diffusion tensor has been found to be significantly lower in the WM surrounding high-grade gliomas than in the WM surrounding metastases, even when the anisotropy has shown no difference.[14] Tensor shape metrics have revealed a relative shift from linear diffusion (prolate tensors) to planar diffusion (oblate tensors) in peritumoral fiber tracts, relative to contralateral tracts.[15] Such examples in which the diffusion tensor is exploited beyond the ADC and FA for purposes of tumoral or peritumoral tissue characterization are only just beginning to be explored.

The directionally encoded color map, with hues reflecting tensor orientation and intensity weighted by FA, provides an aesthetic and informative summary of DTI features throughout the brain in an easily interpreted format. The use of these maps is becoming increasingly common in both basic and clinical research, as well as in purely clinical settings. Our group has described four distinct patterns of tumor-related pathology in WM tracts on FA-weighted, directionally encoded color maps, categorized on the basis of tensor anisotropy and orientation.[16] Unfortunately, these

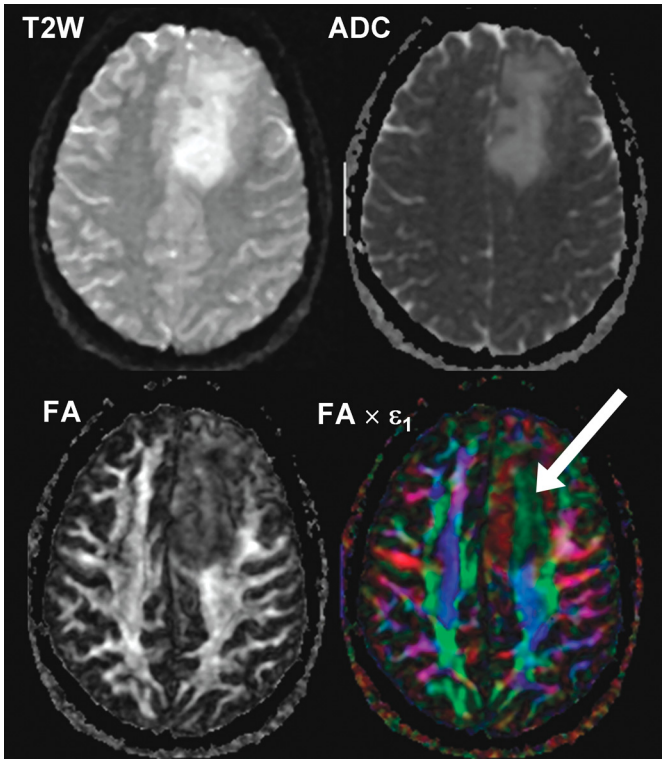

FIGURE 2. T2-weighted (T2W), ADC, FA, and FA-weighted, directionally encoded DTI color maps (FA × ε_1) in a patient with an infiltrating glioma involving the left corona radiata and subcortical U-fibers.[16] This region shows both reduced FA and abnormal color hues (*arrow*), which are not explained by any apparent tract deviation.

patterns rely on subjective assessments of color hue and intensity; although such assessments can be clinically relevant, a more objective, quantitative approach is needed for purposes of further research. Specifically, a formal methodology for analyzing regional distributions of tensor orientations, including measures of regional directional tendency and dispersion, intervoxel coherence, and interhemispheric symmetry, is needed in order to exploit DTI more reliably in the setting of cerebral neoplasm. We are developing various metrics to meet this need,[17] employing the theory and methods of directional statistics.

For example, we have observed several WM tracts infiltrated by bland edema where anisotropy is reduced with no appreciable change in hue on directionally encoded color maps, while several tracts infiltrated by gliomas have had anisotropy reductions accompanied by altered hues that were unexplained by visible tract deviations (FIGS. 1 and 2). Subjective impressions such as these must be validated quantitatively, motivating our development of directional statistical approaches.

REGIONAL METRICS FOR TENSOR ORIENTATION AND SYMMETRY

Directional Histograms ("Rose" Diagrams)

The distribution of major eigenvectors in a region of interest (ROI) can be described in terms of their polar and azimuthal angles (θ and ϕ, respectively) in 3D space.[17]

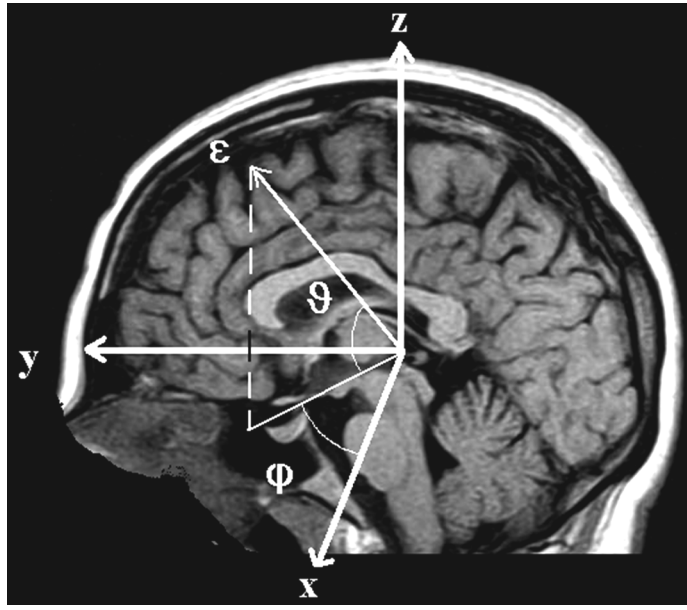

FIGURE 3. The distribution of major eigenvectors in a region of interest can be described in terms of their polar and azimuthal angles (θ and ϕ, respectively) in 3D space.[17] Specifically, the polar angle (θ) denotes the angle between the eigenvector and the *x*-*y* plane, and the azimuthal angle (ϕ) denotes the angle between the eigenvector's projection in the *x*-*y* plane and the *x*-axis.

Specifically, the polar angle (θ) denotes the angle between the eigenvector and the *x*-*y* ("axial") plane, and the azimuthal angle (ϕ) denotes the angle between the eigenvector's projection in the *x*-*y* plane and the *x*-axis (right-left direction) (FIG. 3). Since the WM tract orientations will be mirrored across the cerebral hemispheres, the rotation conventions of ϕ are reversed for regions in the left and the right hemispheres to facilitate symmetry comparisons. The distribution of major eigenvector directions can be calculated for any ROI and subjected to further analysis or displayed as a pair of spherical-coordinate histograms (polar and azimuthal), or "rose" diagrams. In a rose diagram, the arc subtended by each sector bin represents a range of angles, and the length of each bin reflects the frequency of occurrence for that range (FIG. 4). Note that this approach is not rotationally invariant unless θ and ϕ are referenced to anatomically standardized planes. For example, the *y*-*z* ("sagittal")

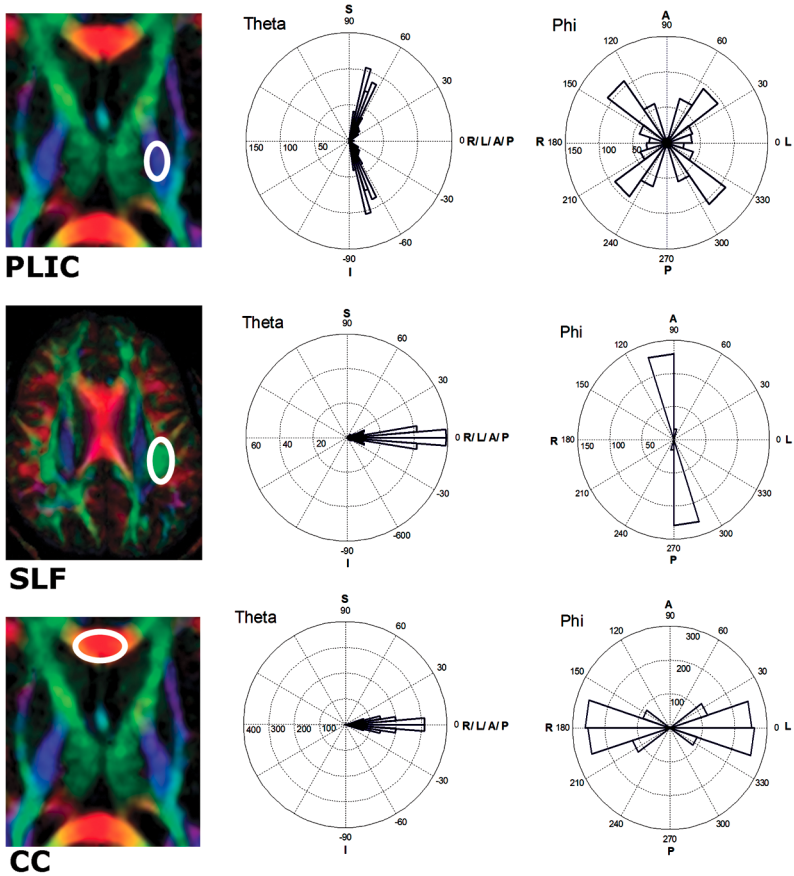

FIGURE 4. Directional histograms (rose diagrams) for posterior limb of internal capsule (PLIC), superior longitudinal fasciculus (SLF), and genu of the corpus callosum (CC) in a normal subject. Note the unique distributions characterizing each of these major tracts. These distributions can be subjected to statistical analysis seeking changes related to pathology.

plane could be defined along the interhemispheric fissure, and the *x*-*y* plane along the intercommissural line and perpendicular to the *y*-*z* plane.

Scatter Matrix

The "preferred" orientation and dispersion of major eigenvectors (analogous to mean and variance, respectively, of eigenvector orientation) in an ROI can also be summarized in terms of the scatter matrix.[17] If ε_{1i} is the major eigenvector of the diffusion tensor for the *i*-th voxel within an ROI containing *n* voxels, then the scatter matrix for the ROI is defined as

$$\boldsymbol{T} = (1/n) \sum_{i=1}^{n} \varepsilon_{1i} \varepsilon_{1i}^{t}$$

where *t* denotes the vector transpose. Like the diffusion tensors themselves, $\boldsymbol{T}$ is a 3×3 diagonally symmetric matrix with its own eigenvectors, $\boldsymbol{t}_1$, $\boldsymbol{t}_2$, and $\boldsymbol{t}_3$, which describe the orientation of the tensor distribution within the ROI.

Symmetry Index

A measure of interhemispheric symmetry for homologous ROIs in the brain may be defined as the dot product of the scatter matrix major eigenvectors for left and right ROIs:[17]

$$S = \boldsymbol{t}_{1\mathbf{L}} \cdot \boldsymbol{t}_{1\mathbf{R}}.$$

A value of *S* approaching unity indicates a high degree of interhemispheric symmetry, while *S* near zero indicates that the left and right tensor distributions are nearly orthogonal. Note that accurate *S* measurements require the *y*-*z* plane to be parallel to the interhemispheric fissure.

CASE EXAMPLES: VASOGENIC EDEMA AND INFILTRATING GLIOMA

Case 1: Vasogenic Edema

A patient with a small (~1 cm) brain metastasis surrounded by a much larger region of vasogenic edema (presumed tumor-free) involving the corona radiata (CR) underwent DTI at 1.5 T using a quadrature head coil and a single-shot, diffusion-weighted spin-echo EPI sequence with diffusion encoding in 23 directions ($b = 0$ and 912 s/mm^2, slice thickness = 3 mm, TR/TE = 4000/72 ms, FOV = 24 cm, matrix = 128×128 interpolated to 256×256, NEX = 4). The diffusion tensor at each voxel was estimated and diagonalized, and maps of FA were generated, using published methods.[18,19] A 3D ROI was manually traced within the edematous CR on FA maps and a homologous ROI was traced in the contralateral CR. Directional histograms for these ROIs (FIG. 5) revealed only nominal changes in tensor distributions, and the symmetry index, calculated as described above, was $S = 0.99$, indicating a high degree of interhemispheric symmetry.

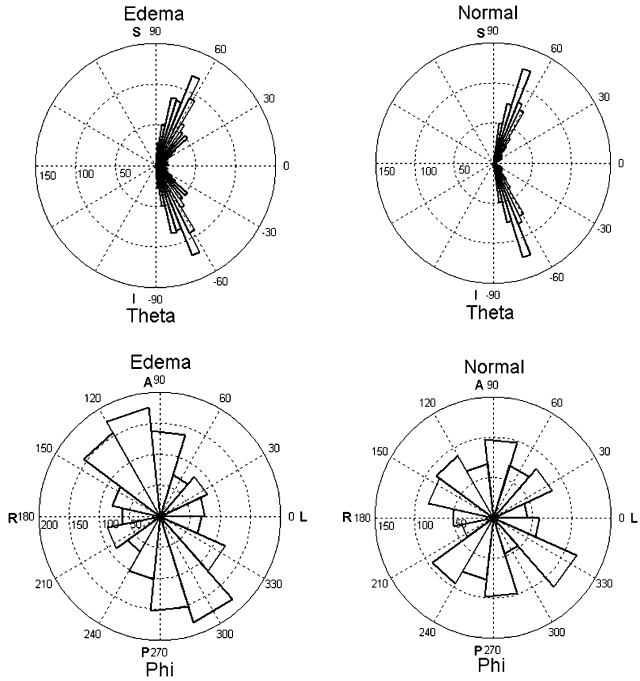

FIGURE 5. ROI rose diagrams of the corona radiata (CR) in case 1, a patient with bland vasogenic edema.[17] (*Left*) Edema ROI. (*Right*) Homologous ROI in normal contralateral CR. Only nominal changes in tensor distributions are evident. Symmetry index $S = 0.99$.

Case 2: Infiltrating Glioma

A patient with an oligodendroglioma (WHO grade II) infiltrating the superior longitudinal fasciculus (SLF) underwent DTI with postprocessing as described for case 1. Directional histograms for homologous SLF ROIs (FIG. 6) revealed more substantial changes in tensor distributions than those seen in the edema case, and the symmetry index was $S = 0.74$, indicating a lesser degree of interhemispheric symmetry.

CONCLUSIONS

These examples serve to demonstrate our approach to the quantitation of regional diffusion tensor distributions using directional statistical methods. Other approaches are certainly possible (e.g., ref. 20). Quantitation along these lines is urgently needed in order to validate the subjective impressions derived from the popular directionally encoded color maps and to enable statistical data analysis whenever relevant changes in fiber tract orientations are postulated or (subjectively) observed. The rose diagrams enable histogram-based analyses of major eigenvector distributions within ROIs;

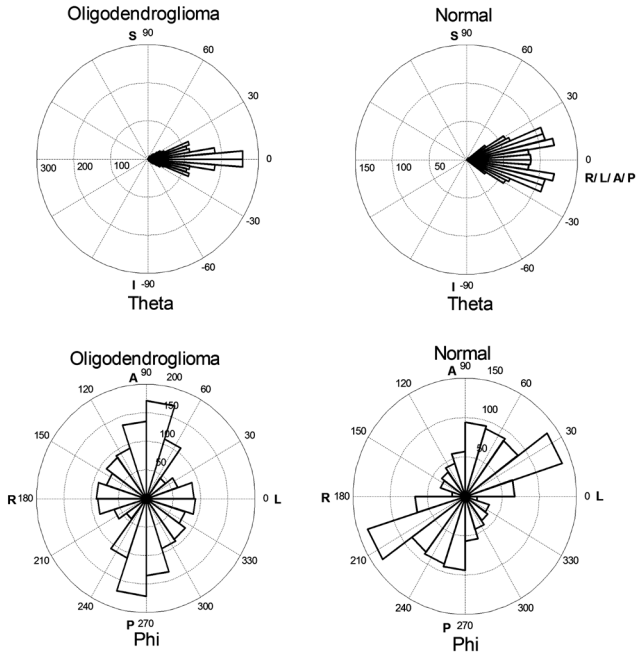

FIGURE 6. ROI rose diagrams of the superior longitudinal fasciculus (SLF) in case 2, a patient with an infiltrating oligodendroglioma.[17] (*Left*) Tumor ROI. (*Right*) Homologous ROI in normal contralateral CR. Changes in tensor distributions are more significant than for bland edema in case 1. Symmetry index $S = 0.74$.

major CNS fiber tracts are expected to have characteristic profiles on these histograms (e.g., FIG. 4), which may be tested for changes resulting from pathology. The symmetry index, derived from the scatter matrix, enables a patient whose disease is limited to one hemisphere to serve as his/her own control. The lesser degree of interhemispheric symmetry that our approach revealed in an infiltrating glioma, as compared to vasogenic edema, suggests that regional analysis of tensor orientation may have an important role to play in this and other problems of tissue characterization. Further study is needed to determine the sensitivity and specificity of our approach in the face of variations in tumor type, grade, location, prior treatment, etc.

REFERENCES

1. BRUNBERG, J.A., T.L. CHENEVERT, P.E. MCKEEVER *et al.* 1995. *In vivo* MR determination of water diffusion coefficients and diffusion anisotropy: correlation with structural alteration in gliomas of the cerebral hemispheres. AJNR Am. J. Neuroradiol. **16:** 361–371.
2. STADNIK, T.W., C. CHASKIS, A. MICHOTTE *et al.* 2001. Diffusion-weighted MR imaging of intracerebral masses: comparison with conventional MR imaging and histologic findings. AJNR Am. J. Neuroradiol. **22:** 969–976.

3. KONO, K., Y. INOUE, K. NAKAYAMA *et al*. 2001. The role of diffusion-weighted imaging in patients with brain tumors. AJNR Am. J. Neuroradiol. **22:** 1081–1088.
4. SINHA, S., M.E. BASTIN, I.R. WHITTLE & J.M. WARDLAW. 2002. Diffusion tensor MR imaging of high-grade cerebral gliomas. AJNR Am. J. Neuroradiol. **23:** 520–527.
5. BASTIN, M.E., S. SINHA, I.R. WHITTLE & J.M. WARDLAW. 2002. Measurements of water diffusion and T1 values in peritumoral oedematous brain. Neuroreport **13:** 1335–1340.
6. TIEN, R.D., G.J. FELSBERG, H. FRIEDMAN *et al*. 1994. MR imaging of high-grade cerebral gliomas: value of diffusion-weighted echo planar pulse sequences. AJR Am. J. Roentgenol. **162:** 671–677.
7. KRABBE, K., P. GIDEON, P. WAGN *et al*. 1997. MR diffusion imaging of human intracranial tumours. Neuroradiology **39:** 483–489.
8. CASTILLO, M., J.K. SMITH, L. KWOCK & K. WILBER. 2001. Apparent diffusion coefficients in the evaluation of high-grade cerebral gliomas. AJNR Am. J. Neuroradiol. **22:** 60–64.
9. LU, S., D. AHN, G. JOHNSON & S. CHA. 2003. Peritumoral diffusion tensor imaging of high-grade gliomas and metastatic brain tumors. AJNR Am. J. Neuroradiol. **24:** 937–941.
10. LU, S., D. AHN, G. JOHNSON *et al*. 2004. Diffusion-tensor MR imaging of intracranial neoplasia and associated peritumoral edema: introduction of the tumor infiltration index. Radiology **232:** 221–228.
11. PROVENZALE, J.M., P. MCGRAW, P. MHATRE *et al*. 2004. Peritumoral brain regions in gliomas and meningiomas: investigation with isotropic diffusion-weighted MR imaging and diffusion-tensor MR imaging. Radiology **232:** 451–460.
12. MAIER, S.E., P. BOGNER, G. BAJZIK *et al*. 2001. Normal brain and brain tumor: multicomponent apparent diffusion coefficient line scan imaging. Radiology **219:** 842–849.
13. FIELD, A.S., A.L. ALEXANDER, V.M. HAUGHTON *et al*. 2002. Effect of vasogenic edema on sensitivity of white matter tractography with diffusion tensor imaging. *In* ASNR 2002 Proceedings, American Society of Neuroradiology 40th Annual Meeting, Vancouver, British Columbia, Canada, May 11–17, 2002; O-269, p. 199.
14. WIEGELL, M.R., J.W. HENSON, D.S. TUCH & A.G. SORENSEN. 2003. Diffusion tensor imaging shows potential to differentiate infiltrating from non-infiltrating tumors. *In* Proceedings of the International Society for Magnetic Resonance in Medicine (ISMRM) 11th Scientific Meeting, Toronto, Ontario, Canada, July 10–16, 2003, p. 2075.
15. ZHANG, S., M.E. BASTIN, D.H. LAIDLAW *et al*. 2004. Visualization and analysis of white matter structural asymmetry in diffusion tensor MRI data. Magn. Reson. Med. **51:** 140–147.
16. FIELD, A.S., A.L. ALEXANDER, Y-C. WU *et al*. 2004. Diffusion tensor eigenvector directional color imaging patterns in the evaluation of cerebral white matter tracts altered by tumor. J. Magn. Reson. Imaging **20:** 555–562.
17. WU, Y-C., A.S. FIELD, M. CHUNG *et al*. 2004. Quantitative analysis of diffusion tensor orientation: theoretical framework. Magn. Reson. Med. **52:** 1146–1155.
18. HASAN, K.M., D.L. PARKER & A.L. ALEXANDER. 2001. Comparison of gradient encoding schemes for diffusion-tensor MRI. J. Magn. Reson. Imaging **13:** 769–780.
19. HASAN, K.M., P.J. BASSER, D.L. PARKER & A.L. ALEXANDER. 2001. Analytical computation of the eigenvalues and eigenvectors in DT-MRI. J. Magn. Reson. **152:** 41–47.
20. SCHWARTZMAN, A., R.F. DOUGHERTY & J.E. TAYLOR. 2004. Comparison of principal diffusion directions using directional statistics. *In* Proceedings of the 10th Annual Meeting of the Organization for Human Brain Mapping, Budapest, Hungary, June 13–17, 2004; WE-300.